

Effect of prestressing on the natural frequency of PSC bridges

Soobong Shin^{*1}, Yuhee Kim^{1a} and Hokyoung Lee^{2b}

¹Department of Civil Engineering, INHA University, 100 Inha-ro, Nam-gu, Incheon 22212, Korea

²Korea Bridge Institute Co., 252 Gilju-ro, Wonmi-gu, Bucheon-si, Gyeonggi-do 14548, Korea

(Received October 8, 2015, Revised November 30, 2015, Accepted December 5, 2015)

Abstract. Depending on the researcher, the effect of prestressing on the natural frequency of a PSC (prestressed concrete) structure appear to have been interpreted differently. Most laboratory tests on PSC beams available showed that the natural frequency is increased appreciably by prestressing. On the other hand, some other references based on field experience argued that the dynamic response of a PSC structure does not change regardless of the prestressing applied. Therefore, the deduced conclusions are inconsistent. Because an experiment with and without prestressing is a difficult task on a full size PSC bridge, the change in natural frequency of a PSC bridge due to prestressing may not be examined through field measurements. The study examined analytically the effects of prestressing on the natural frequency of PSC bridges. A finite element program for an undamped dynamic motion of a beam-tendon system was developed with additional geometric stiffness. The analytical results confirm that a key parameter in changing the natural frequency due to prestressing is the relative ratio of prestressing to the total weight of the structure rather than the prestressing itself.

Keywords: prestressing; natural frequency; PSC bridge; laboratory test; geometric stiffness; total weight

1. Introduction

The dynamic response of a bridge is influenced mainly by its mass or stiffness properties. Variations in the material or sectional properties of a bridge can cause considerable changes in the dynamic response of the structure. Modal data of the natural frequencies and mode shapes are typically obtained and compared to examine any changes in the structure, with natural frequencies being used more widely as a measuring stick (Shin 1994, Tedesco *et al.* 1999). Various and complex analytic methods have been developed to analyze the dynamic response of bridges. Theoretically, such a change in the modal data should be related to the variation of the mass or stiffness properties (Singh *et al.* 2013, Wang *et al.* 2013). In the case a beam is subjected to an additional force due to prestressing, it is generally believed that a change in modal information might be investigated by considering the change in stiffness rather than mass. Theoretical and experimental studies have been carried out to examine the changes in the natural frequencies due

*Corresponding author, Professor, E-mail: sbshin@inha.ac.kr

^aPh.D., Student, E-mail: kimyuhee74@hanmail.net

^bPh.D., Director, E-mail: jangjae@nate.com

to prestressing based on this viewpoint (Goremikins *et al.* 2013, Liu *et al.* 2013, Materazzi *et al.* 2009, Miyamoto *et al.* 2000, Noh *et al.* 2015, Shin *et al.* 2010).

Many laboratory tests have been carried out on PSC specimens to examine the change in the natural frequency of PSC (prestressed concrete) structures (Falati and Williams 1998, Hop 1991, James *et al.* 1964, Nabil and Ross 1996, Ross 1996). All laboratory tests showed that the natural frequency of a PSC beam increased appreciably from those of the RC beam without prestressing. Nabil and Ross (1996) carried out laboratory experiments on test concrete specimens with a hollow section to obtain the dynamic characteristics. By introducing prestressing to the tendon in a parabolic profile, the natural frequency of the test specimen was increased by a maximum of 22%. Saiidi *et al.* (1994) reported a decrease in natural frequency due to the loss of prestressing in measuring the loss of prestressing force of the Golden Valley Bridge. To verify this phenomenon, they also carried out experiments on sample concrete beams in the laboratory and arrived at the same conclusion of an increase in the natural frequency due to prestressing.

On the other hand, some studies insisted that the magnitude of the prestressed force does not affect the natural frequencies of prestressed beams (Hamed and Frostig 2006) or the effect of prestressing can be neglected based on this conclusion (Morassi and Tondon 2008, Whelan *et al.* 2010). Hamed and Frostig (2006) proposed a nonlinear dynamic analysis model that considers the compressive force effect, cable eccentricity and changes in the tension force of a cable. They argued that the classical models have some deficiencies in predicting the variations of the natural frequencies of a prestressed concrete beam and insisted that the magnitude of the prestressing force does not affect the natural frequencies of a PSC beam. On the other hand, they compared their numerical results only with those obtained from other models available in the literature. They did not validate their results with any test data available in the literature. In addition, it is believed that Morassi and Tondon (2008) and Whelan *et al.* (2010) simply adopted the conclusion by Hamed and Frostig (2006) and neglected the prestressing effect in their applications.

These two opposite views to the same physical problem do not appear to have a point of contact. In other words, it can be concluded that the effect of prestressing on the natural frequencies of an actual PSC bridge is not completely understood despite the large body of experimental and theoretical studies. One way of narrowing the gap between these opposite views may be through analytical investigations. Dall'asta (1996, 2000) presented an analytical model for computing the natural frequencies by considering the equilibrium and safety conditions of an I-shaped thin beam with a tendon inside. He used the equation of motion with a frictionless bond between a three-dimensional continuum and a steel tendon. Through an analytical study of the vibrational characteristics of a PSC beam, Dall'asta and Leoni (1999) concluded that the prestressing introduced to a beam-tendon system decreased the natural frequencies, but the influence was negligible. On the other hand, they did not consider the stiffening variations due to the $P-\Delta$ effects in their analytical approach. Law and Lu (2005) calculated the time-domain responses of a prestressed beam and carried out a study to identify the prestressing. Also, Ren *et al.* (2015) carried out numerical simulation study on prestressed precast concrete bridge deck panels using plasticity model. Nevertheless, they limited the application of prestressing to the center of a section, an approach that is seldom used in actual bridges. To reduce the gap between theory and reality, the effective stiffness of a beam was calculated by regressing the natural frequency data obtained from the laboratory experiments and utilizing these results to predict the natural frequencies of a beam. Jaiswal (2008) also investigated analytically the effects of prestressing on the flexural natural frequency of beams through a finite element technique. They concluded that for the beams with a bonded tendon, the prestressing force does not have any appreciable effects

on the first natural frequency while for the beams with an unbonded tendon, the first natural frequency changes with the prestressing force and the eccentricity of the tendon. As a conclusion from these analytical studies, the analytical results are still controversial depending on the mathematical formulations and applied assumptions. Therefore, it is necessary to set up a systematic procedure to examine and apply an analytical approach. First, an adequate analytical method should be developed or selected and its reliability must be examined using test data. The verified analytical method should then be applied to investigate the change in natural frequency of any PSC structure due to prestressing.

This paper proposes a finite element formulation for the undamped dynamic equation of motion that considers the additional geometric stiffness due to prestressing. The developed finite element program was examined using the laboratory test data available in the literature and was proven to be reliable throughout the study. The analytical results matched the measured increases in natural frequencies with tendon prestressing applied to the laboratory test specimens. The verified finite element program was then applied to the analytical models of actual PSC bridges to examine the variation of the natural frequency due to the application of prestressing. The analytical results from the developed finite element program showed negligible changes in the natural frequency in the actual PSC bridges. This controversial results of the application to laboratory PSC specimens and those to an actual size PSC bridge are reviewed in detail and show that a key parameter contributing this opposite phenomena is the relative ratio of the applied prestressing force to the total weight of the structure rather than the prestressing itself. Some analytical results related to this conclusion are summarized and reviewed in this paper.

2. Dynamic equation of motion with prestressing effects

2.1 Equation of motion of a prestressed beam

If the material property of a prestressing tendon is homogeneous and isotropic, the tendon may receive the same tension throughout its length. The stress at the beam may be divided into the normal stress by the beam deformation and the geometric stress by tension in the tendon. The principle of virtual work can be applied to the beam-tendon system. Dall'asta and Leoni (1999) derived the following equation

$$\begin{aligned} & \int_V \mathbf{S} \cdot \hat{\mathbf{E}} \, dV + \tau(a) \hat{a} L_0 + \int_V \mathbf{T}_0 \cdot \mathbf{U}^T \hat{\mathbf{U}} \, dV + \frac{\tau_0}{L_0} \int_0^L (\mathbf{I} - \mathbf{g}_c \otimes \mathbf{g}_c) \cdot (\mathbf{U}^h \mathbf{h}' \otimes \hat{\mathbf{U}}^h \mathbf{h}') \, dV \\ & = \int_V \rho_0 (\mathbf{b} - \ddot{\mathbf{u}}) \cdot \hat{\mathbf{u}} \, dV + \int_S \mathbf{t} \cdot \hat{\mathbf{u}} \, dS \end{aligned} \quad (1)$$

where \mathbf{S} = a stress tensor of the beam, $\tau(a)$ = uniform tendon stress due to beam deformation, \mathbf{T}_0 = a Cauchy stress tensor, τ_0 , L_0 = initial tendon stress and initial length of the tendon, ρ_0 = unit mass of the beam, \mathbf{b} , \mathbf{t} = body force and traction force applied to the beam, respectively, a = tendon axial strain, \mathbf{U} , \mathbf{h} , \mathbf{g}_c = the deformation gradient of the beam, the position vector of a tendon at its reference configuration, and the tangent unit vector of the initial tendon path, respectively, \mathbf{U}^h = the deformation gradient of the tendon path, and $\hat{\mathbf{E}}$, $\hat{\mathbf{u}}$, \hat{a} = a virtual strain tensor, virtual displacements of the beam, and virtual strain of the tendon, respectively.

The equation of motion by Dall'asta and Leoni (1999) may reflect the actual situation more

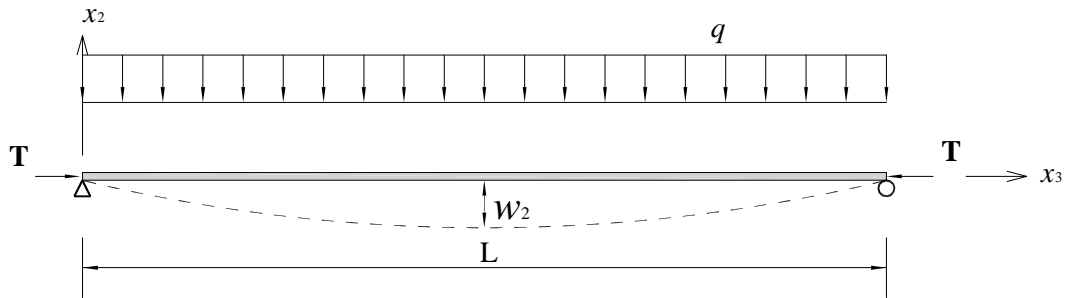


Fig. 1 Beam with prestressing and its straight reference configuration

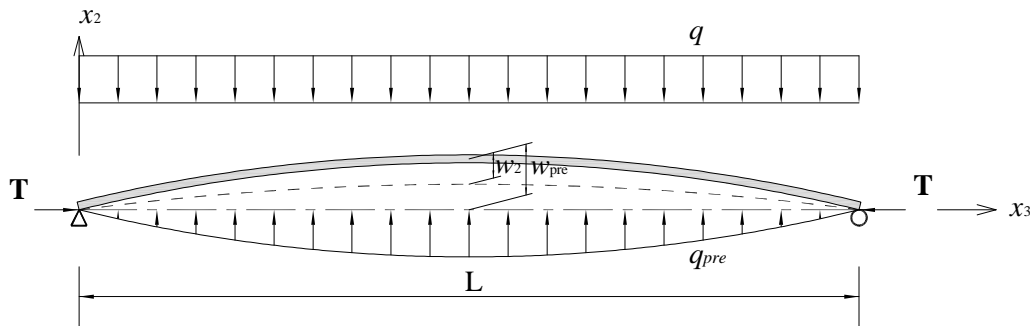


Fig. 2 Beam with initial displacement due to prestressing

closely than the conventional form because it considers the tendon profile along the beam. As it still does not consider the initial beam deformation due to the prestressing force, however, the third term containing the Cauchy stress tensor reduces the stiffness of the system when its reference configuration is straight, as shown in Fig. 1. As a result, the third term decreases the total stiffness of the system though the geometric stiffness of the fourth term because the tendon force increases the total stiffness, leading to a decrease in the natural frequencies.

2.2 Linear geometric stiffness with initial beam deformation

Tendons in actual PSC beams were arranged with constant eccentricity or in a parabolic profile to the downward direction, so that an initial upward vertical displacement opposite to the applied loading direction can occur. This initial deformation may determine the direction of buckling and also develop a $P-\Delta$ moment with a different sign from that of the flexural moment due to the applied loads. Consequently, the flexural stiffness of the beam may be increased.

Fig. 2 presents a beam with an upward distributed load due to a prestressing force in the tendon. The distributed load due to the prestress q_{pre} can develop vertical displacement w_{pre} and also a corresponding moment of $T w_{pre}$ due to the axial force T . The moment $T w_{pre}$ may have the opposite direction to the moment due to the applied load q . If the beam returns to the original horizontal position with the opposite forces, the beam stiffness can be considered to have been increased. Therefore, although the deflection due to the applied load is in a range of $w < w_{pre}$, the stiffness term T_0 of Eq. (1) has a positive sign, whereas it has a negative sign if $w > w_{pre}$.

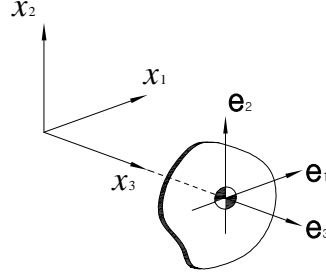


Fig. 3 Coordinate system of a beam cross section

2.3 Undamped dynamic equation of motion

A new finite element formulation for the undamped dynamic equation of motion is derived. The Euler-Bernoulli beam theory was applied to the first term of Eq. (1) by neglecting the shear deformation. In the second term of Eq. (1), a transformed section was applied in the first term to simplify the stiffness equation of the model. In the third and fourth terms related to the linear geometric stiffness of the beam and the tendon, respectively, the model is simplified by limiting the displacement, w , only to the vertical direction.

With the curvature θ' in the Euler-Bernoulli beam model, the first term of Eq. (1) can be modified as Eq. (2). Fig. 3 shows the coordinate system for a beam cross section in the following equations.

$$\int_0^L \mathbf{D} \theta' \cdot \hat{\theta}' dx_3 = \mathbf{d}^T \left(\int_0^L \mathbf{B}^T \mathbf{D} \mathbf{B} dx_3 \right) \hat{\mathbf{d}} \quad (2)$$

where $\theta' = (\theta'_1 \theta'_3)^T$, $\mathbf{d} = (w_{2i} \theta_{1i} \theta_{3i} w_{2j} \theta_{1j} \theta_{3j})$ with $\theta'_1 = w''_2$, $\theta'_3 =$ the first derivative of the torsional rotation, $\mathbf{D} = \text{diag}[EI_{22}, GJ]$, and \mathbf{B} = the strain-displacement matrix with shape functions \mathbf{N} and their derivatives defined by

$$\mathbf{B} = \begin{bmatrix} \frac{d^2}{dx_3^2} N_1(x_3) & \frac{d^2}{dx_3^2} N_2(x_3) & 0 & \frac{d^2}{dx_3^2} N_3(x_3) & \frac{d^2}{dx_3^2} N_4(x_3) & 0 \\ 0 & 0 & \frac{d}{dx_3} N_5(x_3) & 0 & 0 & \frac{d}{dx_3} N_6(x_3) \end{bmatrix} \quad (3)$$

where the Hermitian polynomials are used for the shape functions $N_1 \sim N_4$ and Lagrangian polynomials for $N_5 \sim N_6$, respectively.

The third term of Eq. (1), the geometric stiffness due to an axial force, can be simplified to Eq. (4).

$$\int_0^L T w'_2 \hat{w}'_2 dx_3 = \kappa \mathbf{d}^T \left(\int_0^L T \mathbf{N}_G^T \mathbf{N}_G dx_3 \right) \hat{\mathbf{d}} \quad (4)$$

where κ = the coefficient determining the sign of the geometric stiffness defined by Eq. (5) when an axial force T is applied and \mathbf{N}_G is defined as the derivatives of the shape functions by Eq. (6), respectively.

$$\kappa = \begin{cases} -1 : & w_2 \geq w_{2pre} \\ +1 : & w_2 < w_{2pre} \end{cases} \quad (5)$$

where w_{2pre} = upward deflection due to prestressing.

$$\mathbf{N}_G = \begin{bmatrix} \frac{d}{dx_3} N_1(x_3) & \frac{d}{dx_3} N_2(x_3) & 0 & \frac{d}{dx_3} N_3(x_3) & \frac{d}{dx_3} N_4(x_3) & 0 \end{bmatrix} \quad (6)$$

The fourth term of Eq. (1), the geometric stiffness of a taut string due to the tension by prestressing can be simplified to Eq. (7) by considering w_2' as the only strain component.

$$\int_0^L \frac{T}{\ell^3} w_2' \hat{w}_2' dx_3 = \mathbf{d}^T \left(\int_0^L \frac{T}{\ell^3} \mathbf{N}_{Gc}^T \mathbf{N}_{Gc} dx_3 \right) \hat{\mathbf{d}} \quad (7)$$

where $\ell = \sqrt{(x_{c2}')^2 + 1}$ and \mathbf{N}_{Gc} is defined as the derivatives of the shape functions by Eq. (8).

$$\mathbf{N}_{Gc} = \begin{bmatrix} \frac{d}{dx_3} N_1(x_3) & 0 & 0 & \frac{d}{dx_3} N_3(x_3) & 0 & 0 \end{bmatrix} \quad (8)$$

The force term after neglecting the body force can be expressed as Eq. (9).

$$-\int_V \rho_0 \ddot{\mathbf{u}} \cdot \hat{\mathbf{u}} dV + \int_S \mathbf{t} \cdot \hat{\mathbf{u}} dS = \int_0^L \mathbf{N}^T \mathbf{q} \cdot \hat{\mathbf{d}} dx_3 - \int_0^L \mathbf{N}^T \mathbf{L} \mathbf{N} \ddot{\mathbf{d}} \cdot \hat{\mathbf{d}} dx_3 = \left(\mathbf{f} - \int_0^L \mathbf{N}^T \mathbf{L} \mathbf{N} \ddot{\mathbf{d}} dx_3 \right) \cdot \hat{\mathbf{d}} \quad (9)$$

where \mathbf{q} = the applied distributed load vector, and \mathbf{L} = the matrix for mass per unit length.

By eliminating the virtual displacement on both sides as an arbitrary one, the final undamped equation of motion can be derived as

$$\mathbf{M} \ddot{\mathbf{d}}(t) + (\mathbf{K}_B + \delta \mathbf{K}_G + \mathbf{K}_{Gc}) \mathbf{d}(t) = \mathbf{f} \quad (10)$$

where \mathbf{K}_B = the normal stiffness, $\delta \mathbf{K}_G$ = the geometric stiffness due to axial force and \mathbf{K}_{Gc} = the geometric stiffness of a taut string due to the tension by prestressing, respectively.

$$\mathbf{K}_B = \int_0^L \mathbf{B}^T \mathbf{D} \mathbf{B} dx_3, \quad \delta \mathbf{K}_G = \kappa \int_0^L T \mathbf{N}_G^T \mathbf{N}_G dx_3, \quad \mathbf{K}_{Gc} = \int_0^L \frac{T}{\ell^3} \mathbf{N}_{Gc}^T \mathbf{N}_{Gc} dx_3 \quad (11)$$

$$\mathbf{f} = \int_0^L \mathbf{N}^T \mathbf{q} dx_3, \quad \mathbf{M} = \int_0^L \mathbf{N}^T \mathbf{L} \mathbf{N} dx_3 \quad (12)$$

If an external force is not applied, then Eq. (10) can be transformed to the eigenvalue problem of Eq. (13) to solve for the natural frequencies and mode shapes of the beam-tendon system.

$$(\mathbf{K}_B + \delta \mathbf{K}_G + \mathbf{K}_{Gc}) \boldsymbol{\phi}_j = \omega_j^2 \mathbf{M} \boldsymbol{\phi}_j \quad (13)$$

3. Validation of the proposed model with the laboratory test data

Modal information obtained from the proposed equation given in Eq. (13) was compared with

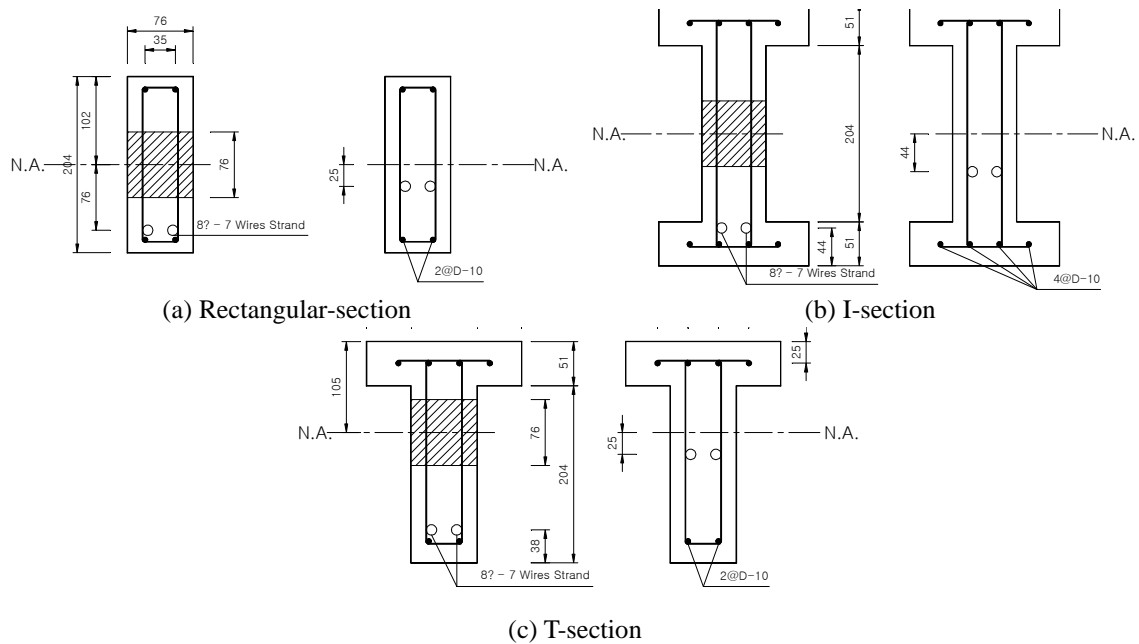


Fig. 4 Sectional properties of the tested specimens (mm)

that from the available laboratory experiments carried out by Nabil and Ross (1996). Although there are other available laboratory experimental results, such as those by Hope (1991) and Sadii (1994), only those presented by Nabil and Ross (1996) were compared in the present paper because their data included various sectional shapes. The types of specimens for the experiments included rectangular, T-shape and I-shape sections, as shown in Fig. 4. All the specimens used for the tests had a length of 5m with seven wire strands, 8mm in diameter. The tendons were placed in a parabolic profile along the length. For each type of section, the identified natural frequency of the first mode was compared with the frequency calculated from the proposed method with variations in the prestressing force. Each specimen had a web opening at the midspan. On the other hand, this effect of web opening on the natural frequency can be neglected according to Navil and Ross (1996)'s experimental results.

Fig. 5 compares the variations of the first natural frequency of each sectional type, obtained from the experiment with those from the proposed model with increasing prestressing force. The two sets of results of rectangular- and I-section coincide very well throughout the range applied prestressing forces. As the prestressing force is increased, the first natural frequency increases almost linearly. On the other hand, the first natural frequency of the T-section increases almost linearly as in the other cases but with a constant gap between the experimental data and the analytically proposed model, as shown in Fig. 5(c). Because a rough calculation made using a commercial software package without any prestressing confirmed the validity of the proposed method, the authors consider that the information computed in the original paper might contain some error, such as the specimen size. From the results for three different sectional types, there is a clear trend of a linear increase in the first natural frequency with increasing prestressing force. Among the tested cases, such a trend was most pronounced in the rectangular section and smallest in the I-section.

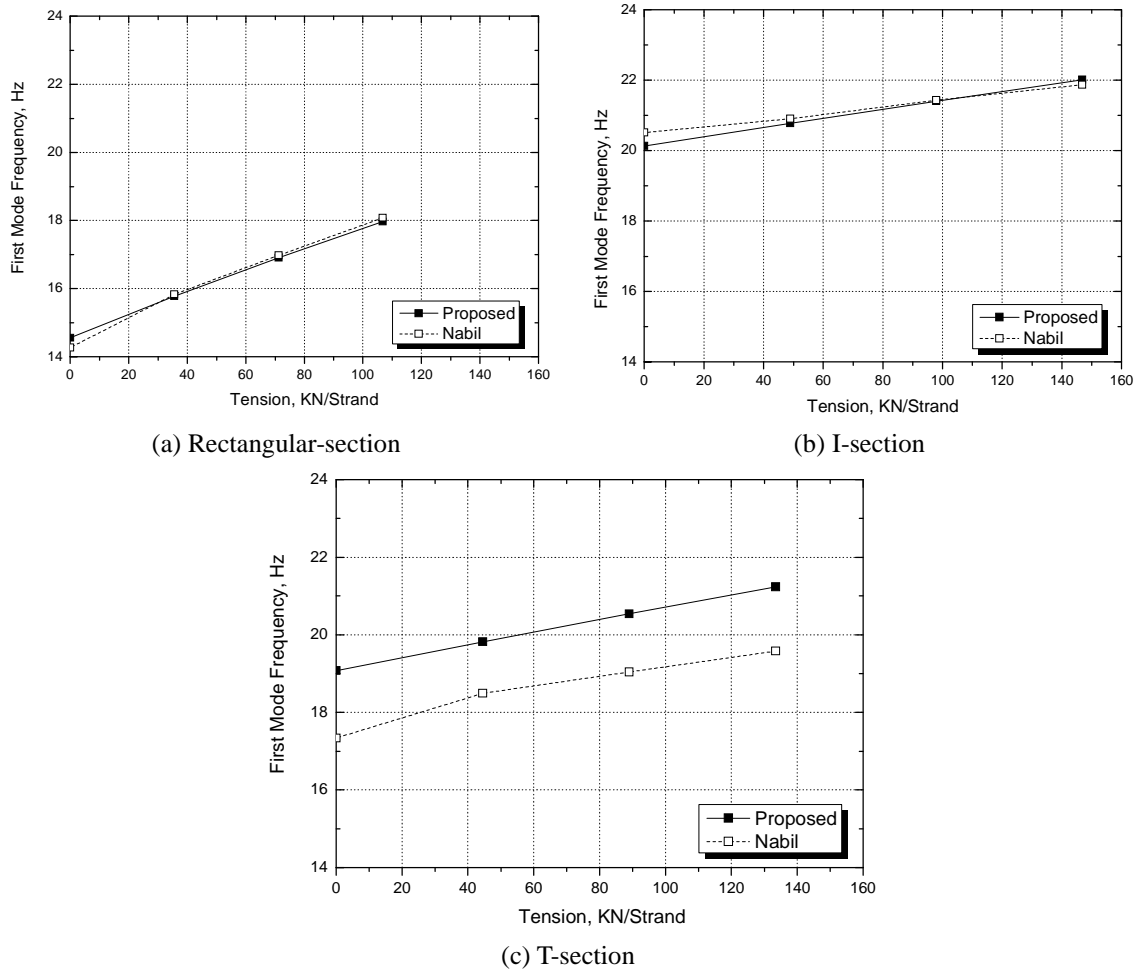


Fig. 5 Comparison of the experimental results with the calculated frequencies

Table 1 Material and sectional properties of the model bridges

	A-20	A-23	A-25	B-25
f_c' (MPa)		35		40
Girder				
Slab			27	
Density (kg/m ³)			2,500	
I (m ⁴)	0.7476		1.0295	1.1237
J (m ⁴)	0.0433		0.0426	0.0467

Table 2 Natural frequencies by the proposed finite element model

	A-20	A-23	A-25	B-25
f_0 (Hz)	9.017	6.403	6.171	6.541
f_p (Hz)	9.118	6.515	6.262	6.640
f_p / f_0 (grillage analysis)	1.011	1.018	1.015	1.015

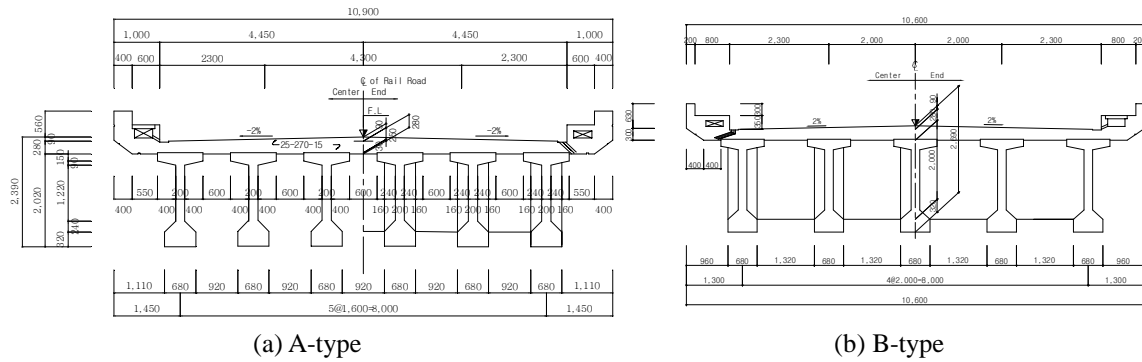


Fig. 6 Cross-sections of the model bridges (mm)

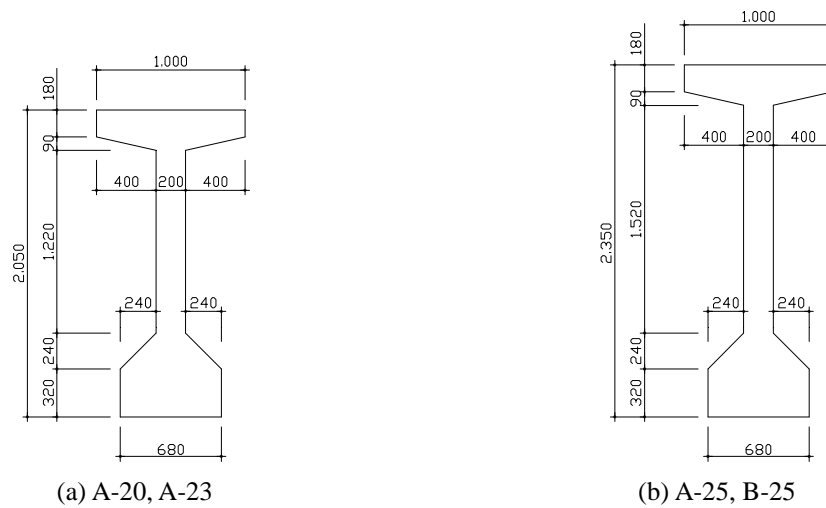


Fig. 7 Details of the girder beam sections (mm)

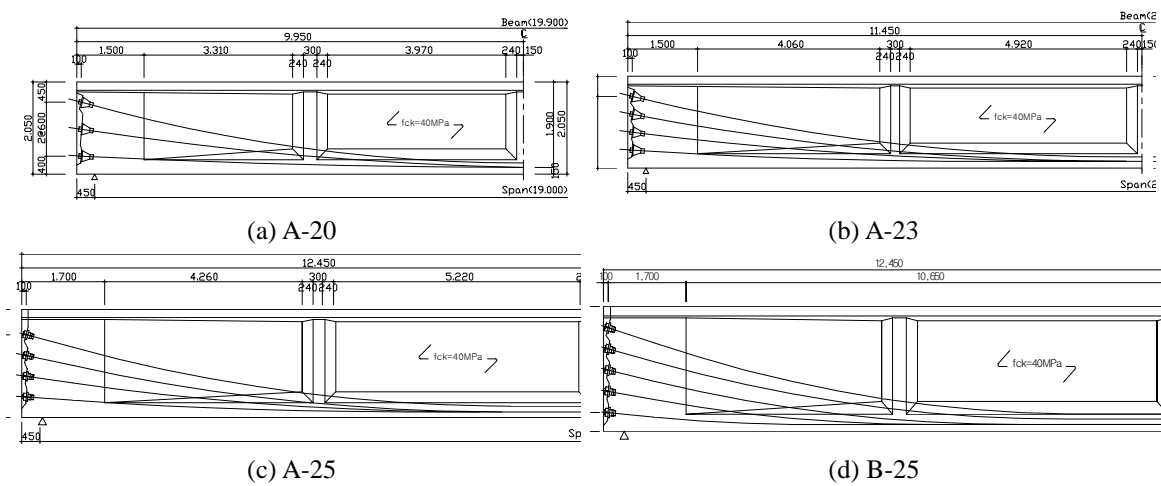


Fig. 8 Details of the tendon layouts (mm)

Table 3 Ratio of the prestressing to the total weight

	Nabil and Ross (1996) specimen [Fig. 4]			PSC railway bridges [Figs. 6-8]			
	rectangle	I-section	T-section	A-20	A-23	A-25	B-25
Total weight (kN)	1.91	4.21	3.07	4,450	5,118	5,788	5,251
Sum of prestressing (kN)	103.80	146.85	133.50	4,817	6,515	6,380	7,475
Prestressing / Weight	54.35	34.88	43.49	1.08	1.27	1.10	1.42

4. Applications to PSC bridges

To examine the effects of prestressing on actual bridges, sample studies using the proposed model have been carried out on PSC bridges designed for an actual railway system. For the sample studies with the designed bridges, prestressings were applied to the designed values.

4.1 Sectional and material properties of the bridges

Four different types of PSC bridges were designed with sections, as shown in Fig. 8-Fig. 10 for the A-type and B-type. The width of the slab was fixed to 10.9 m for the A-type and 10.6 m for the B-type. The A-type models have 6 PSC beams. The simply-supported span length between the centers of the piers was 20 m, 23 m and 25 m, depending on the model. Comparatively, the B-type has 5 PSC beams with a simply-supported span length of 25 m. Table 1 summarizes the material and sectional properties of each girder type. The mass of each girder is comprised of the mass of the slab and the following items: rail (120 kg/m), ballast (800 kg/m) and sleeper (6 EA/m: 762 kg/m).

4.2 Natural frequency of the PSC railway bridges

Grillage models were applied to analyze the designed four types of simply supported railway PSC bridges shown in Figs. 6-8. Table 2 lists the natural frequencies calculated from the proposed finite element model for each type of bridge, where f_0 and f_p denote the natural frequency without and with prestressing, respectively. Table 2 shows that the evaluated effect of the prestressing is less than 2%, which is different from the trend in Fig. 5.

One clear observation is that the proposed finite element program can model successfully the two opposite results regarding the effect of prestressing on the natural frequency. In other words, although the results from the two different group opinions appear to be quite opposite, the fundamental physical phenomenon can be explained on the same basis.

4.3 Point of contact between the two opposite opinions

Because the natural frequency is affected by the variation of stiffness and the mass properties of a structure, the influence of each property on the change in natural frequency should be investigated, particularly when the stiffness property varies due to the applied prestressing. Table 3 compares the relative ratio of the prestressing force to the total weight of the structure for the Nabil and Ross (1996) laboratory tests and for actual size PSC bridges. Surprisingly, Table 3 clearly

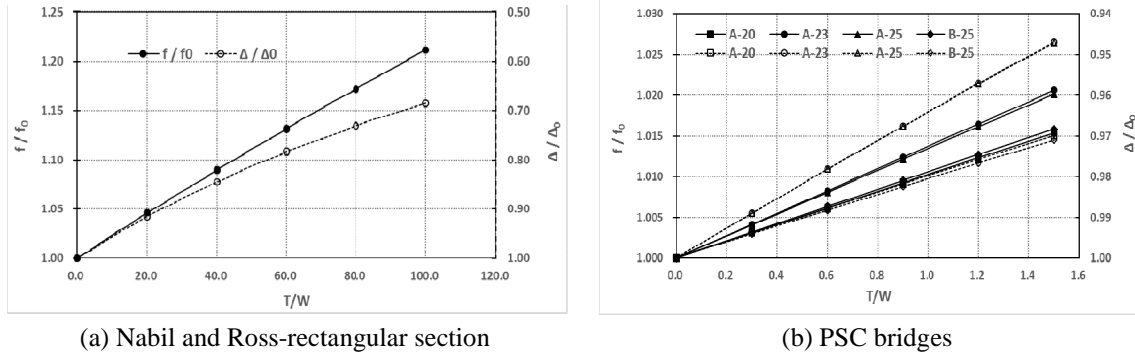


Fig. 9 Variation of the natural frequency and vertical deflection with the relative increase in prestressing to the total weight

shows the difference in the two cases. The relative ratio of prestressing to the total weight of the laboratory test specimens of Nabil and Ross (1996) was in the range of 34.88~54.35, whereas that of PSC bridges was in 1.08~1.42, which are quite small. In other words, the variation of the natural frequencies for the laboratory tests and the actual cases were studied under totally different environments in terms of mass.

The variation of the natural frequency depending on the ratio of the prestressing to the total weight of a structure was examined by carrying out a simulation study with the analytical model for the rectangular section of Nabil and Ross (1996). The solid line in Fig. 9(a) shows a linear increase in the natural frequency with increasing ratio of the prestressing to the total weight (T/W) from zero to 100. In the same figure of Fig. 9(a), the dotted line shows the decrease in vertical deflection at the middle span when a concentrated load is applied at the middle of the simply supported PSC beam. The right-hand-side vertical coordinate indicates the ratio of deflection with prestressing T to that without prestressing. The decrease in deflection is due to the increase in stiffness due to prestressing, as explained in Eq. (13) but is not so linear as the case of the variation of natural frequency. When the ratio of prestressing to the total weight T/W is 100, the natural frequency increases approximately 22% and the deflection decreases by more than 30%, which are considerable changes. On the other hand, Fig. 9(b) shows the analytical results of the increase in natural frequency and the decrease in deflection with increasing ratio of prestressing to the total weight T/W up to 1.5. In this region, the variations of the natural frequency and the deflection of the actual PSC bridges are almost negligible, as listed in Table 3. In Fig. 9(b), the dotted lines show the decrease in deflections of the bridges as the prestressing increases.

Overall, it is true that the natural frequency changes with increase of prestressing but the change ratio is strongly dependent on the relative amount of prestressing to the total weight of a structure. Therefore, even if a considerable change in the natural frequency can be observed from normal laboratory tests, it is natural that the change in natural frequency in an actual PSC structure is negligible.

5. Conclusions

The study examined the effects of prestressing on the natural frequencies of PSC beams and

PSC bridges. A finite element formulation was introduced based on the principle of virtual work to define the modal equation of motion of a beam-tendon system. In the formulation of stiffness, two terms of the geometric stiffness due to axial force and the geometric stiffness of a taut string due to the tension by prestressing were added to the original structural stiffness. The developed finite element program was examined through applications to laboratory experimental data and could model the considerable change in natural frequency due to the increase in prestressing quite well. In addition, the program also could prove that the change in natural frequency of an actual PSC bridge can be negligible, as insisted by the other part of engineers. Therefore, the current study proves that both opposite opinions regarding the change in natural frequency due to prestressing are true based on the same physical phenomenon. A simulation study on a simply supported PSC beam with the variation of prestressing suggest that the key parameter of the problem is the relative ratio of the prestressing to the total weight of the structure rather than prestressing itself.

In conclusion, when the ratio of prestressing to the total weight of the structure is small as an actual size PSC structure, the changes in natural frequency and the vertical deflection can be negligible, even though the prestressing is totally lost. Therefore, the change in natural frequency or vertical deflection cannot be a good indicator of safety or serviceability performance of a PSC bridge. In other words, different indices for the safety and serviceability performance of a PSC bridge should be investigated.

Acknowledgments

This research was supported by Basic Science Research Program through the National Research Foundation of Korea (NRF) funded by the Ministry of Education, science and technology (NRF-2012R1A1A2008974) and INHA University

References

- Dall'Asta, A. (1996), "On the coupling between three dimensional bodies and slipping cables", *Int. J. Solid. Struct.*, **33**(24), 3587-3600.
- Dall'Asta, A. (2000), "Dynamics of elastic bodies prestressed by internal slipping cables", *Int. J. Solid. Struct.*, **37**(25), 3421-3438.
- Dall'Asta, A. and Leoni, G. (1999), "Vibrations of beams prestressed by internal frictionless cables", *J. Sound. Vib.*, **222**(1), 1-18.
- Falati, S. and Williams, M.S. (1998), *Vibration tests on a model post-tensioned concrete floor: Interim report*, Report No. OUEL 2155/98, University of Oxford, Dept. Eng. Sci., UK.
- Goremikins, V., Rocens, K., Serdjus, D. and Gaile, L. (2013), "Experimental determination of natural frequencies of prestressed suspension bridge model", *Constr. Sci.*, **14**, 32-37.
- Grace, N.F. and Ross, B. (1996), "Dynamic characteristics of post-tensioned girders with web openings", *J. Struct. Eng.*, **122**(6), 643-650.
- Hamed, E. and Frostig, Y. (2006), "Natural frequencies of bonded and unbonded prestressed beams-prestress force effects", *J. Sound. Vib.*, **295**(1), 28-39.
- Hop, T. (1991), "The effect of degree of prestressing and age of concrete beams on frequency and damping of their free vibration", *Mater. Struct.*, **24**(3), 210-220.
- Jaiswal, O.R. (2008), "Effect of prestressing on the first flexural natural frequency of beams", *Struct. Eng. Mech.*, **28**(5), 515-524.
- James, M.L., Smith, G.M. and Lutes, L.D. (1964), "Dynamic properties of reinforced and prestressed

- concrete structural components”, *ACI J. Proc.*, **61**(11), 1359-1381..
- Law, S.S. and Lu, Z.R. (2005), “Time domain responses of a prestressed beam and prestress identification”, *J. Sound. Vib.*, **288**(4), 1011-1025.
- Liu, H.B., Wang, L.L., Tan, G.J. and Cheng, Y.C. (2013), “Prestress force effect on natural frequencies of simply supported beams”, *Appl. Mech. Mater.*, **275**, 1172-1175.
- Materazzi, A.L., Breccolotti, M., Ubertini, F. and Venanzi, I. (2009), “Experimental modal analysis for assessing prestress force in PC bridges: a sensitivity study”, *Proceedings of the International Modal Analysis Conference (IOMAC 2009)*, June.
- Miyamoto, A., Tei, K., Nakamura, H. and Bull, J.W. (2000), “Behavior of prestressed beam strengthened with external tendons”, *J. Struct. Eng.*, **126**(9), 1033-1044.
- Morassi, A. and Tonon, S. (2008), “Dynamic testing for structural identification of a bridge”, *J. Bridge Eng.*, **13**(6), 573-585.
- Noh, M.H., Seong, T.R., Lee, J. and Park, K.S. (2015), “Experimental investigation of dynamic behavior of prestressed girders with internal tendons”, *Int. J. Steel Struct.*, **15**(2), 401-414.
- Ren, W., Sneed, L.H., Yang, Y. and He, R. (2014), “Numerical simulation of prestressed precast concrete bridge deck panels using damage plasticity model”, *Int. J. Concrete Struct. Mater.*, **9**(1), 45-54.
- Saïdi, M., Douglas, B. and Feng, S. (1994), “Prestress force effect on vibration frequency of concrete bridges”, *J. Struct. Eng.*, **120**(7), 2233-2241.
- Shin, S. (1994), *Damage detection and assessment of structural systems from measured response*, Ph.D. Thesis, University of Illinois at Urbana-Champaign, Illinois.
- Shin, S., Koo, M.S., Lee, H.K. and Kwon, S.J. (2010), “Variation of eigen-properties of a PSC bridge due to prestressing force”, *Proceedings of the Fifth International IABMAS Conference*, Philadelphia, July.
- Singh, B.P., Yazdani, N. and Ramirez, G. (2013), “Effect of a time dependent concrete modulus of elasticity on prestress losses in bridge girders”, *Int. J. Concrete Struct. Mater.*, **7**(3), 183-191.
- Tedesco, J.W., McDougal, W.G. and Ross, C.A. (1999), *Structural dynamics theory and applications*, California, Addison-Wesley.
- Wang, T.H., Huang, R. and Wang, T.W. (2013), “The variation of flexural rigidity for post-tensioned prestressed concrete beams”, *J. Marine Sci. Tech.*, **21**(3), 300-308.
- Whelan, M.J., Gangone, M.V., Janoyan, K.D., Hoult, N.A., Middleton, C.R. and Soga, K. (2010), “Wireless operational modal analysis of a multi-span prestressed concrete bridge for structural identification”, *Smart Struct. Syst.*, **6**(5-6), 579-593.